ACS APPLIED POLYMER MATERIALS

pubs.acs.org/acsapm Article

Dynamics of Poly(cyclohexene carbonate) as a Function of Molar Mass

Marianna Spyridakou, Christina Gardiner, George Papamokos, Holger Frey,* and George Floudas*

Cite This: ACS Appl. Polym. Mater. 2022, 4, 3833−3843 Read Online

ACCESS | Metrics & More | Article Recommendations | Supporting Information

ABSTRACT: Stereoregular poly(cyclohexene carbonate) (PCHC) homopolymers were prepared via copolymerization of cyclohexene oxide and carbon dioxide (CO_2) using (*R*,*R*)-(salcy)-CoCl and bis(triphenylphosphine)iminium chloride as a catalyst. The homopolymers had molar masses in the range of 4800−33,000 g mol^{-1} and relatively narrow dispersity after careful fractionation, as required for the molecular dynamics investigation. We employed differential scanning calorimetry and dielectric spectroscopy, the latter as a function of temperature and pressure, for investigating the thermal properties and the molecular dynamics, respectively. The segmental dynamics in the vicinity of the liquid-to-glass temperature was very complex. The dual segmental processes were inseparable by decreasing the temperature or by increasing the pressure. Based on DFT calculations of the dipole moment, they were ascribed to different stereo sequences of the PCHC backbone. The limiting glass temperature, T_g, for very high molar masses was ∼125 °C. The high T_g value obtained herein well justifies its application as a CO_2-based alternative for polystyrene (PS) in a variety of materials based on block copolymers. Moreover, fragility increased with increasing molar mass with values intermediate to poly(styrene) and poly(cyclohexyl methacrylate). The flexible cyclohexyl group in PCHC undergoing intramolecular chair-to-chair conversion increases the packing ability and consequently decreases the fragility. PCHC is a brittle material because it lacks entanglements even for the higher molar masses investigated herein, which is relevant for application as a PS substitute. Within the investigated range of molar masses, the dependences of the terminal relaxation times, τ_{NM}, and of the zero-shear viscosity, η_o, on the molar mass, M, are $\tau_{NM}/\tau_{SM} \sim M^{3.2}$ and $\eta_o \sim M^{1.4}$, revealing an intermediate behavior between Rouse and entangled chains.

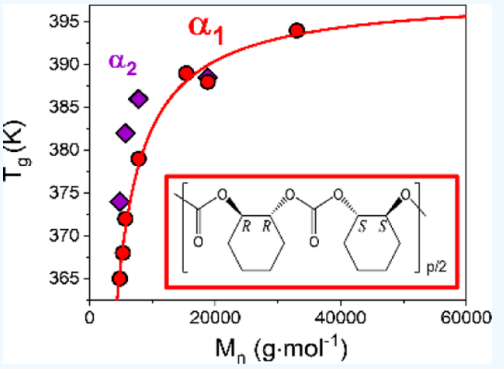

KEYWORDS: *carbon dioxide synthesis, aliphatic polycarbonate, glass temperature, segmental dynamics, rheology*

INTRODUCTION

Carbon dioxide, the main greenhouse gas, offers exciting possibilities for polymer synthesis due to its low cost and natural abundance. The copolymerization of carbon dioxide with epoxides, leading to aliphatic polycarbonates, was introduced by Inoue in 1969.[1] Meanwhile, a large variety of new catalyst systems has been developed, resulting in higher molar masses and high content of carbonate linkages that provide improved control of both molar masses and dispersities.[2,3] Poly(cyclohexene carbonate) (PCHC), an aliphatic polycarbonate based on CO_2 and cyclohexene oxide (CHO), was used in several works to demonstrate the efficiency and selectivity of different catalyst systems.[3−8] Because of its rather high glass temperature (T_g) (reported values are in the range from 115 to 120 °C),[6,9−12] PCHC is viewed as a rigid and biodegradable, CO_2-based alternative for polystyrene (PS) in block copolymers. Consequently, PCHC has been employed for a variety of polymer architectures, including complex block copolymers and hyperbranched polycarbonates.[13−17]

Although PCHC plays an important role in polycarbonate chemistry (as a high T_g polymer), its physical properties are largely unexplored. Wu et al. investigated isotactic PCHC, which exhibits a high melting point within the temperature range 215−230 °C.[5] Furthermore, Gakh et al. evaluated the physical properties of PCHC, albeit with a limited molecular mass (M_n) of 8000 g mol^{-1} and rather high dispersity. The thermal and mechanical properties as well as the dynamic mechanical behavior of PCHC were studied by Koning and Darensbourg et al.[18] These authors studied a PCHC homopolymer of 42000 g mol^{-1}, albeit with very broad molar mass distribution ($Đ$ = 6). They observed a T_g at 115 °C and determined the mechanical properties, for example, elongation at break (1−2%) and Young's modulus (3.6

Received: February 18, 2022
Accepted: April 14, 2022
Published: April 25, 2022

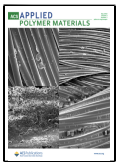

https://doi.org/10.1021/acsapm.2c00299
ACS Appl. Polym. Mater. 2022, 4, 3833−3843

GPa), showing that PCHC is a stiff and brittle material. In addition, the authors concluded that the backbone of PCHC is even less flexible than that of bisphenol-A (BPA)-based aromatic polycarbonates. This was attributed to the chair−chair conformational transitions of the cyclohexane group.[18] Despite these early efforts, the molecular dynamics of PCHC remains unexplored, as well as the viscoelastic properties that largely determine the mechanical response at ambient temperature. Moreover, the dependence of the liquid-to-glass temperature on molar mass has not been studied systematically (almost all studies rely on a single homopolymer sample with a very broad distribution of molar masses).

To address these open issues, we synthesize a series of PCHC homopolymers with molar masses in the range from 4800 to 33,000 g mol^{-1} and with relatively narrow dispersities. We employ differential scanning calorimetry and dielectric spectroscopy (DS), the latter as a function of temperature and pressure, for investigating the thermal properties and the molecular dynamics. In this way, we establish the molar mass dependence of the glass temperature as well as the molecular processes and their dynamics acting both below and above T_g. We show that the molecular dynamics at the segmental level is complex and are influenced by the stereochemistry. To this end, we employed density functional theory calculations of the dipole moments of the different conformers. In addition, rheology is employed, aiming at estimating the critical molar mass above which entanglements play a role. We find that homopolymers with molar masses below 33,000 g mol^{-1} lack a clear plateau in the storage modulus, suggesting brittle behavior for lower molar masses.

EXPERIMENTAL SECTION

Materials. All solvents and reagents were utilized as obtained unless otherwise stated. CHO [Acros Organics, Pittsburgh, PA (USA) or Alfa Aesar, Kandel (Germany)] was distilled over CaH_2 under reduced pressure prior to use. Carbon dioxide (>99.99%) was purchased from Westfalen AG (Münster, Germany). Bis(triphenylphosphine)iminium chloride ([PPN]Cl) was received from abcr GmbH. (*R*,*R*)-(salcy)-Co(III)Cl was prepared as described by Ford et al.[19] All solvents were received from Sigma-Aldrich, Fischer Chemical (Pittsburgh, PA, USA), and Honeywell (Morris Plaines, NJ, USA) and used without further purification. All other reagents were purchased from Sigma-Aldrich or Arcos Organics (Pittsburgh, PA, USA). Deuterated solvents were obtained from Deutero GmbH (Kastellaun, Germany).

PCHC Synthesis. The synthesis procedures for $PCHC_{108}$ are described below. CHO (6.0 mL, 59 mmol, 1 equiv), (*R*,*R*)-(salcy)-CoCl (CoSalen, 30.3 mg, 0.047 mmol, 0.008 equiv), and [PPN]Cl (27.2 mg, 0.047 mmol, 0.008 equiv) were filled in an autoclave, equipped with a stirring-bar, in an inert argon atmosphere. Subsequently, the reaction mixture was stirred at a carbon dioxide pressure of 50 bar at 50 °C for 41 h. The crude product was dissolved in dichloromethane, and the catalyst was deactivated with 10 mL of 5% vol HCl solution in methanol at 60 °C. The product was precipitated by using ice-cold methanol as a nonsolvent. The precipitated product was collected by centrifugation at 4500 rpm at 0 °C for 10 min. The precipitation procedure was repeated twice. Repeated fractionation was carried out to improve the dispersity of the samples used in this study by slowly adding cold methanol. The obtained colorless solid was finally dried under reduced pressure 10^{-3} mbar at 40 °C for 24 h.

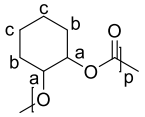

^{1}H NMR (300 MHz, chloroform-d): δ [ppm] 4.62 (s, 2H, a), 2.08 (m, 2H, b), 1.67 (m, 2H, b), 1.43−1.33 (m, 4H, c). M_n(THF, PS) = 18,800 g mol^{-1}; $Đ$ = 1.23.

To obtain homopolymers of different molar masses, the amount of catalyst was varied. Moreover, adding a small amount of dry toluene in the synthesis was observed to lead to higher molar masses.

NMR Analysis. ^{1}H and ^{13}C NMR spectra were recorded using a Bruker 400 spectrometer (Bruker Corporation, Billerica, MA, USA) operated at 300 MHz (^{1}H NMR), 400 MHz (^{1}H NMR), and 75 MHz (^{13}C NMR) at 23 °C, and the chemical shifts are given in parts per million (ppm). All spectra are referenced to residual solvent signals.

Size Exclusion Chromatography. Size exclusion chromatography (SEC) measurements were accomplished in tetrahydrofuran (THF) (1 mL/min, 30 °C) on a SDV column set from polystyrene standards (PSS) (SDV 103, SDV 105, and SDV 106), equipped with UV (254 nm) and RI detectors. Calibration was carried out using PSS, typical for PCHC characterization.

FT-IR Analysis. Fourier transform infrared spectroscopy (FT-IR) spectra were recorded using an iS10 FT-IR spectrometer (Thermo Scientific, Waltham, MA, USA) equipped with a diamond ATR unit.

Temperature-Modulated Differential Scanning Calorimetry. Temperature-modulated differential scanning calorimetry (TM-DSC) measurements were made for PCHC homopolymers with the same Q2000 (TA Instruments) using cooling/heating rates in the range of 10 to 1 K min^{-1} and oscillation periods from 20 to 150 s. A specific rate/period pair was employed for each measurement according to[20]

$$\beta = \frac{\Delta T_g}{cP} 60 \text{ s/min} \quad (1)$$

Here, β is the cooling/heating rate, ΔT_g is the range of T_g, c is the number of cycles across the T_g width, and P is the oscillation period. For PCHC, ΔT_g = 20 K and the number of cycles used was 5 for efficient deconvolution of the modulated signal. The rate/period pairs used were as follows: 20 s, 10 K min^{-1}; 40 s, 5 K min^{-1}; 60 s, 2 K min^{-1}; 150 s, 1.3 K min^{-1}. TM-DSC measurements were made within the temperature range from 303 to 423 K.

Dielectric Spectroscopy. DS measurements as a function of temperature (T) and pressure (P) were performed with a Novocontrol Alpha frequency analyzer. The T-dependent measurements at ambient pressure were performed within the range from 203 to 443 K in steps of 5 K for frequencies in the range from 10^{-2} to 10^7 Hz. The sample cell consisted of two electrodes, 20 mm in diameter and 50 μm in thickness, maintained by Teflon spacers. Samples were prepared as melts by pressing the electrodes to the spacer thickness under vacuum. The P-dependent protocol involved measurements from 413 to 463 K in steps of 10 K in a Novocontrol pressure cell. The pressure setup consisted of a temperature-controlled cell, a hydraulic closing press with an air pump, and an air pump for hydrostatic test pressure. The preparation of the sample capacitor began with the sample pressed under vacuum between 20 mm diameter electrodes and a thickness of 50 μm maintained with a Teflon spacer. Subsequently, the capacitor was wrapped with Teflon tape and arranged inside a Teflon ring in order to prevent the flow of silicon oil into the sample. The silicone oil (DOW CORNING 550 Fluid) is the liquid that uniformly transmits pressure to the sample. The isothermal measurements were made with temperature stability better than 0.1 K and pressure stability better than 2 MPa. The complex dielectric permittivity, $\varepsilon^* = \varepsilon' - i\varepsilon''$, where ε' is the real part and ε'' is the imaginary part, was obtained as a function of frequency, ω, temperature, T, and pressure, P, that is, (T,P,ω).[21,22] The analysis of the DS curves was based on the empirical equation of Havriliak and Negami (HN)[23]

$$\epsilon^*_{HN}(T, P, \omega) - \epsilon_\infty(T, P) = \frac{\Delta\epsilon(T, P)}{[1 + (i\omega\tau_{HN}(T, P))^m]^n} \quad (2)$$

where $\varepsilon_\infty(T,P)$ is the high-frequency permittivity, $\tau_{HN}(T,P)$ is the characteristic relaxation time of the equation, $\Delta\varepsilon(T,P) = \varepsilon_o(T,P) - \varepsilon_\infty(T,P)$ is the relaxation strength, and m and n (with limits $0 < m, mn \leq 1$) describe, respectively, the symmetrical and asymmetrical

https://doi.org/10.1021/acsapm.2c00299
ACS Appl. Polym. Mater. 2022, 4, 3833−3843

broadening of the distribution of relaxation times. A term describing the conductivity contribution was included in the fitting procedure as $\sigma_o(T)/i\varepsilon_f\omega$, where σ_o is the dc conductivity and ε_f is the permittivity of free space. From τ_{HN}, the relaxation times at maximum loss, τ_{max}, were obtained analytically from the HN equation as follows

$$\tau_{max} = \tau_{HN} \sin^{-1/m}\left[\frac{\pi m}{2(1+n)}\right]\sin^{1/m}\left[\frac{\pi mn}{2(1+n)}\right] \quad (3)$$

These relaxation times correspond to the relaxation times of the segmental process. At lower frequencies, ε'' rises because of the conductivity ($\varepsilon'' = \sigma/(\omega\varepsilon_f)$). This conductivity contribution has also been taken into account during the fitting process. Except for the measured ε'', the derivative of the real part of the dielectric permittivity, ε', ($d\varepsilon'/d \ln \omega \approx (2/\pi)\varepsilon''$) was used in the analysis of the dynamic behavior.

Rheology. A TA Instruments rheometer, AR-G2, with a magnetic bearing that allows for nanotorque control was used to record the viscoelastic properties of PCHC as a function of molar mass. Measurements were made with the environmental test chamber as a function of temperature. Samples were prepared on the lower plate of the 8 mm diameter parallel plate geometry. Temperature control was achieved within 0.1 K with a nitrogen convection oven. The linear and nonlinear viscoelastic regions were determined by the strain amplitude dependence of the complex shear modulus $|G^*|$ at ω = 10 rad s^{-1}. The storage (G') and loss (G'') shear moduli were measured as a function of frequency, ω, within the range $10^{-1} < \omega < 10^2$ rad·s^{-1} at several temperatures from 393 to 453 K. Subsequently, the complex viscosity (η^*) follows as $\eta^* = |G^*|/\omega$. Master curves were constructed by using the time−temperature superposition principle. The shift factors, α_T, were fitted according to the Williams−Landel−Ferry (WLF) equation as $\log \alpha_T = -C_1(T - T_r)/C_2 + (T - T_r)$, where C_1 and C_2 are empirical parameters at the reference temperature (T_r). Subsequently, the data were shifted horizontally (by factors α'_T) to achieve iso-friction conditions.

Computational Methods. Initially, (1*R*,2*R*)-*trans*-DMCC and (1*S*,2*S*)-*trans*-DMCC, the two mirror-image monomers, were minimized at the DFT-ωB97X-D/aug-cc-pVDZ[24] level of theory and basis set. The initial structures were the lowest energy conformers predicted by Yoshida and co-workers in their recent work.[25] The results of the minimization were adopted as building blocks of the stereoregular structures of isotactic [meso, (*R*,*R*)(*R*,*R*)] and syndiotactic [racemo, (*R*,*R*)(*S*,*S*)] *trans*-poly(cyclohexene carbonate) dimers. Subsequently, both dimers were optimized at the same level of theory and basis set, and their dipole moments were calculated. The Gaussian 16 R.A.03[26] software package was employed for all computations in this work. The calculations in this paper were run on the FASRC Cannon cluster supported by the FAS Division of Science Research Computing Group at Harvard University.

RESULTS AND DISCUSSION

Polymer Synthesis and Characterization. PCHC was synthesized via copolymerization of CHO and carbon dioxide (CO_2) using CoSalen and [PPN]Cl as a catalyst system (Scheme 1).

The well-known catalyst system CoSalen and [PPN]Cl was chosen due to the perfectly alternating incorporation of carbon dioxide and CHO. This catalyst system suppresses ether defects that can be formed by side reactions in catalytic polymerization. The polycarbonate structure is supported by the ^{1}H NMR spectrum (Figure S1, Supporting Information) (absence of undesired poly(cyclohexene oxide) signals at 3.46 ppm).[27] Another potential side reaction of the CO_2 and epoxide copolymerization is the undesired formation of cyclic carbonates. However, since CHO is a rigid monomer, the formation of the thermodynamically favored cyclic carbonates is suppressed. FT-IR spectroscopy (Figure 1) demonstrates the absence of five-membered cyclic carbonates. Exclusively, the carbonyl stretch vibration of the aliphatic polycarbonates at 1738 cm^{-1} was identified. An additional carbonyl band indicative of the cyclic carbonates at around 1800 cm^{-1} was not observed.

Scheme 1. Synthesis of PCHC Using CoSalen and [PPN]Cl as a Catalyst System

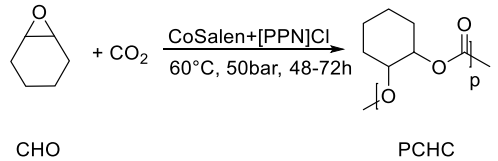

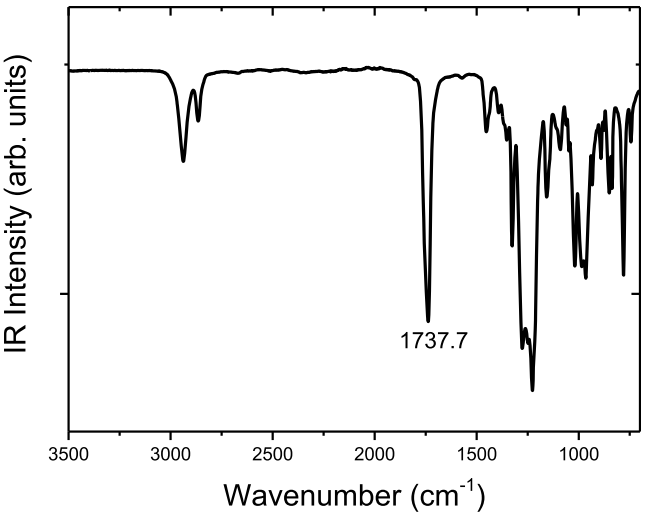

Figure 1. IR spectrum of the crude product of $PCHC_{108}$.

Molar masses were determined using SEC with THF as an eluent and PS as a standard (Figure 2 and Table 1). The SEC curves show a bimodal distribution. This is explained by the initiation process. The chloride ion of the [PPN]Cl initiates CHO/CO_2 copolymerization, but additionally, water traces in the commercially available CO_2 also act as an initiator leading to bimodal distribution (Figure 2). Higher molar masses show larger dispersities (Figure 2) due to the different initiation modes. Molar masses in the range from 4800 to 33,000 g·mol^{-1} with respective dispersities in the range from 1.05 to

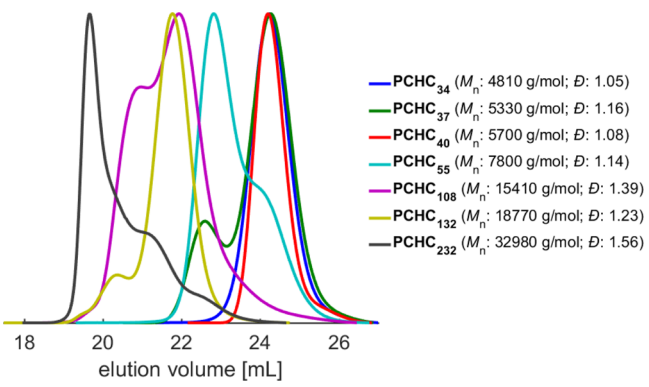

Figure 2. SEC traces of the PCHC homopolymers (eluent: THF; standard: PS).

https://doi.org/10.1021/acsapm.2c00299
ACS Appl. Polym. Mater. 2022, 4, 3833−3843

Table 1. Molecular Characteristics of the Synthesized PCHC Homopolymers

sample	M_n (g mol^{-1})[a]	$Đ$[a]
$PCHC_{34}$	4800	1.05
$PCHC_{37}$	5300	1.16
$PCHC_{40}$	5700	1.08
$PCHC_{55}$	7800	1.14
$PCHC_{108}$	15,400	1.39
$PCHC_{132}$	18,800	1.23
$PCHC_{232}$	33,000	1.56

[a]Determined by SEC using THF as the eluent and PS as the standard.

1.56 could be achieved. To improve the dispersity, fractionation was performed as specified in the Experimental Section.

To investigate the stereochemistry of the polymers, ^{13}C NMR inverse-gated characterization was performed on three samples (Table S1). Figure S2 in the Supporting Information shows the ^{13}C inverse-gated spectrum of $PCHC_{108}$ and the assigned triads.[2] The ^{13}C NMR spectrum of PCHC reveals that the [mmm] + [mmr] tetrad signals show similar integral intensity as those of the remaining tetrads, indicative of the formation of an atactic polymer (Figure S2 and Table S1).[2] Samples $PCHC_{37}$ and $PCHC_{232}$ reveal nearly the same amount of triads, supporting again the formation of an atactic polymer (Table S1).

Computational Results. The computational study aims to calculate the dipole moment as a function of stereochemistry. The calculated values of the dipole moments of isotactic and syndiotactic *trans*-poly(cyclohexene carbonate) dimers are 0.7 and 3.8 D, respectively. Their structures and their dipole moments are shown in Figure 3. Substituted cyclohexanes depend strongly on the stereochemistry of the synthesized compounds regarding their dipole moments.[28] Here, the syndiotactic *trans*-PCHC dimer has a low value of dipole moment because it is highly symmetric, and the existing electric dipoles cancel each other. On the contrary, the isotactic isomer does not have a highly symmetric structure, and its dipole moment is high (Cartesian coordinates of the minimized structures are available in the Supporting Information). The presence of syndiotactic (of low dipole moment) and some atactic (of high dipole moment) dimers along the backbone is expected to influence the dipolar dynamics of the homopolymers (see below).

Thermodynamic Properties. Homopolymer thermodynamics were studied by following the temperature dependence of the reversing heat capacity with respect to frequency by TM-DSC. Some representative results of $PCHC_{34}$ are shown in Figure 4a, whereas the normal DSC is depicted in Figure S3, Supporting Information. The figure depicts the reversing heat capacity signal, c_p, for different modulation periods. As anticipated, T_g increases with decreasing modulation period, which is more evident in the derivative of c_p with respect to temperature. The frequency dependence of the molecular dynamics will be explored in more detail by DS (below). Figure 4b depicts the characteristic length scale at the glass temperature, ξ_α (~1.6 nm), obtained by Donth equation[29]

$$N_\alpha = \frac{\xi_\alpha^3 \rho N_A}{M} = \frac{RT_g^2 \Delta\left(\frac{1}{C_V}\right)}{M(\delta T)^2} \approx \frac{RT_g^2 \Delta\left(\frac{1}{C_p}\right)}{M(\delta T)^2} \quad (4)$$

Here, N_α is the number of repeat units within a cooperative rearranging domain, R is the gas constant, N_A is the Avogadro number, M is the molar mass of the repeat unit, $\Delta(1/C_p) = 1/C_p^{glass} - 1/C_p^{liquid}$ is calculated from the width ΔT of the glass temperature, and $\delta T = \Delta T/2.5$ is the temperature fluctuation obtained from the width of the glass temperature.

Molecular Dynamics as a Function of Temperature and Pressure. To access the molecular dynamics, we employed DS as a function of temperature at ambient pressure and as a function of pressure at some selected temperatures. Some representative dielectric loss curves for $PCHC_{34}$ are shown in Figure 5 together with the fitting to a summation of HN functions (the fitting procedure of the DS data is explained in the Supporting Information with respect to Figure S4). At high temperature, the figure depicts the segmental relaxation times that conform to the usual Vogel–Fulcher–Tammann (VFT) equation

$$\tau = \tau_o^{\#} \exp\left(\frac{B}{T - T_o}\right) \quad (5)$$

where $\tau_o^{\#}$ is the relaxation time in the limit of very high temperatures, B is the activation parameter, and T_o is the

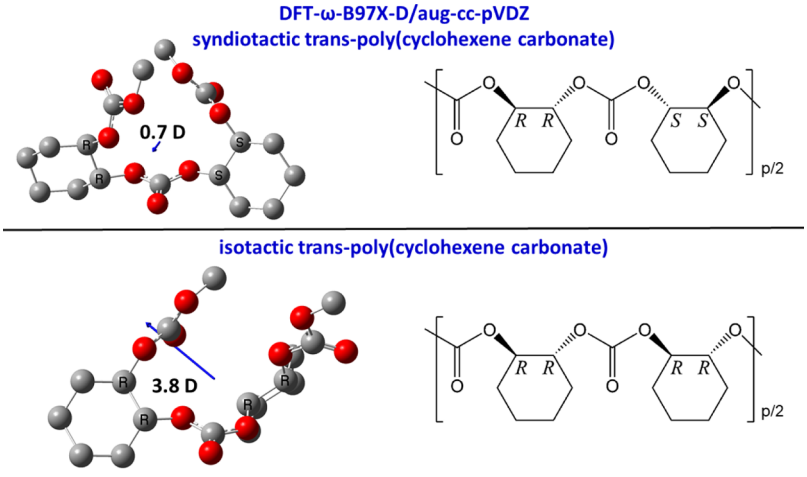

Figure 3. Minimized structures and dipole moments of syndiotactic (top) and isotactic (bottom) *trans*-poly(cyclohexene carbonate). The vectors indicate the direction of the dipole moment. p is the degree of polymerization.

https://doi.org/10.1021/acsapm.2c00299
ACS Appl. Polym. Mater. 2022, 4, 3833−3843

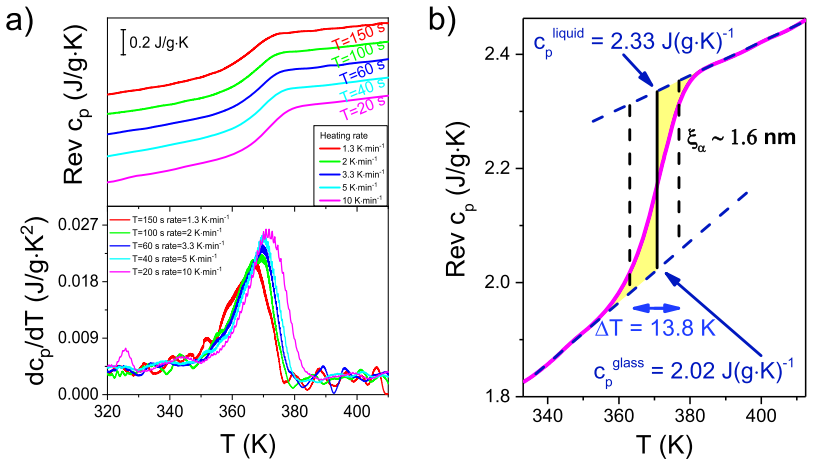

Figure 4. (a) (Top) Temperature dependence of the reversing heat capacity for $PCHC_{34}$, obtained from TM-DSC at different periods of modulation as indicated. Data are shifted vertically for clarity. (Bottom) Derivative of reversible heat capacity with respect to temperature plotted as a function of temperature for different periods of modulation. (b) Temperature dependence of the reversing heat capacity for $PCHC_{34}$ for an oscillation period of T = 20 s and the characteristic length related with the glass temperature, ξ_α.

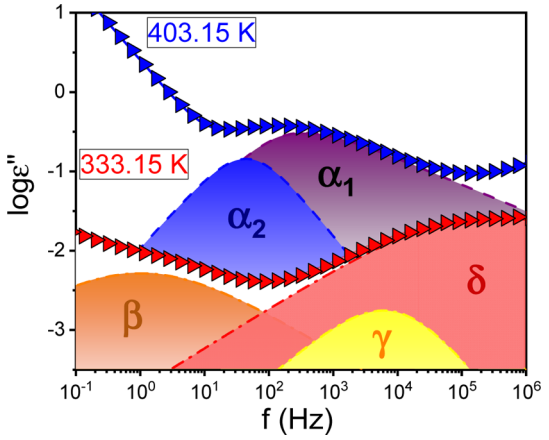

Figure 5. Dielectric loss curves of $PCHC_{34}$ are shown at two temperatures as indicated. At 430.15 K, the shadowed purple and blue areas correspond to simulations of the α_1 and α_2 processes. At 333.15 K, the shadowed orange, yellow, and red areas are simulations of the HN function for the three processes in the glassy state (β, γ, and δ).

"ideal" glass temperature. The parameters of the different processes at and above T_g are summarized in Table 2. We note here that all processes reflect motions of the −COOR dipole that is affected by the cyclohexene ring.

The extracted relaxation times for all processes in $PCHC_{34}$ are shown in the activation diagram of Figure 6. Here, the

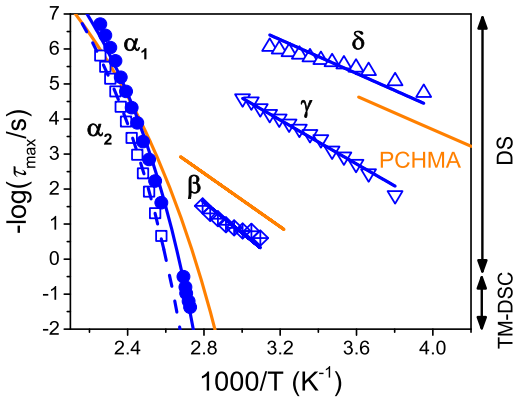

Figure 6. Activation plot of the relaxation times for the different processes of $PCHC_{34}$. Starting from higher temperatures: (squares) α_2 process, (circles) α_1 segmental process, (crossed rhombi) β process, (down triangle) γ process, and (up triangle) δ process. TM-DSC data are also shown. The lines represent fits to the VFT and Arrhenius equations (see text). The relaxation processes of PCHMA are plotted with orange lines.[39]

Table 2. VFT Parameters for the Segmental Relaxations, α_1 and α_2 Obtained from DS and DSC for PCHC Homopolymers with Different Molar Masses

	sample	$-\log(\tau_o/s)$[a]	B (K)	T_o (K)	T_g^{DS} (K)
α_1 process	$PCHC_{34}$	−14	2660 ± 55	292 ± 2	365 ± 1
	$PCHC_{37}$	−14	2665 ± 80	295 ± 3	368 ± 1
	$PCHC_{40}$	−14	2810 ± 110	295 ± 4	372 ± 1
	$PCHC_{55}$	−14	2650 ± 60	307 ± 2	379 ± 1
	$PCHC_{132}$	−14	2230 ± 10	327 ± 1	388 ± 1
α_2 process	$PCHC_{34}$	−14	2730 ± 30	300 ± 1	374 ± 1
	$PCHC_{37}$				
	$PCHC_{40}$	−14	2350 ± 90	318 ± 3	380 ± 1
	$PCHC_{55}$	−14	2520 ± 30	319 ± 1	386 ± 1
	$PCHC_{132}$	−14	2555 ± 40	318 ± 1	389 ± 1

[a]Value held fixed.

https://doi.org/10.1021/acsapm.2c00299
ACS Appl. Polym. Mater. 2022, 4, 3833−3843

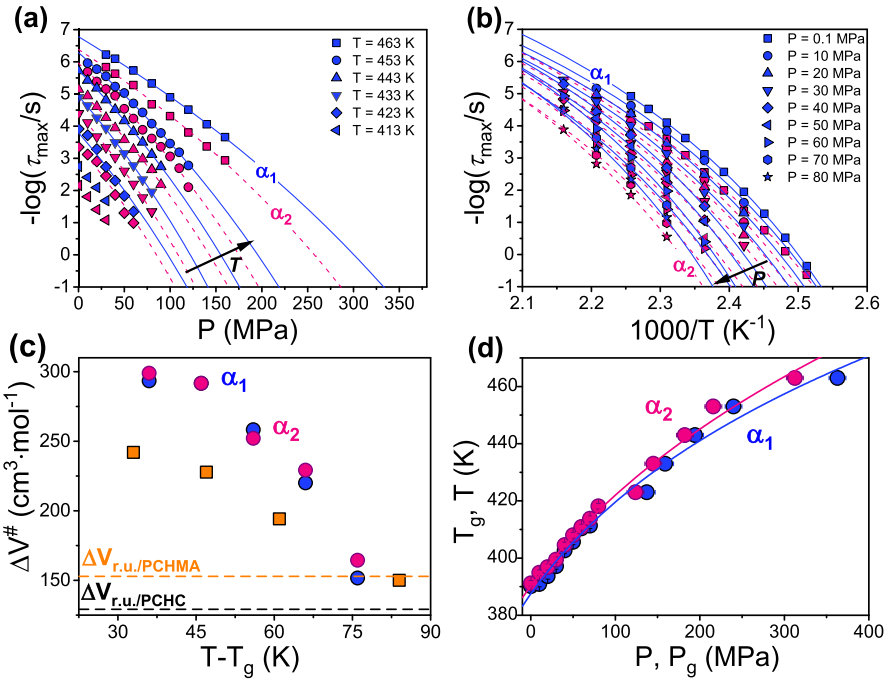

Figure 7. (a) Pressure dependence of the α_1 (blue symbols) and α_2 (pink symbols) processes at temperatures from 413 to 463 K, as indicated. The solid and dashed lines are fits to eq 7. (b) Temperature dependence of the same segmental processes under "isobaric" conditions. Pressure increases along the arrow. The solid and dashed lines are fits to eq 5. (c) Apparent activation volume of PCHC at 0.1 MPa as a function of temperature. Blue and pink symbols represent the α_1 and α_2 segmental processes, respectively. The corresponding volume for PCHMA is also included (orange symbols). The horizontal dashed lines give the corresponding repeat unit volumes. (d) Pressure dependence of T_g and temperature dependence of P_g for the α_1 segmental process (blue) and the α_2 segmental process (pink). Data are obtained from the "isothermal" and "isobaric" representations at t = 100 s. The solid lines represent fits with eq 9.

investigated homopolymer is compared with poly(cyclohexyl methacrylate) (PCHMA), a thoroughly studied polymer,[30−39] as its repeat unit bears strong similarities (a carboxyl group and a cyclohexyl/cyclohexene ring). The relaxation processes of PCHMA are also included in the activation plot.

At higher temperatures, the segmental process is the dominant mode of relaxation with a contribution from the ionic conductivity at lower frequencies. A second process (α_2) of lower effective dielectric strength ($T\Delta\varepsilon_{\alpha1} \sim 525$ K; $T\Delta\varepsilon_{\alpha2} \sim 135$ K) appears on the low-frequency side of α_1 (Figure 5). Since the polymer is atactic, the majority of repeat units will have alternate units resembling syndiotactic units possessing low dipole moments ($\mu \sim 0.7$ D/dimer unit). On the other hand, some isotactic units will appear to have higher dipole moment ($\mu \sim 3.8$ D/dimer unit). Because of the proximity of the two segmental relaxations (Figure 5) and the pressure investigation below, we associate α_2 with the relaxation of the latter units. Hence, the dual segmental processes are attributed to the different stereochemistry of the backbone units. Further pressure-dependent measurements will provide additional insight into their origin.

The dielectric strength of the segmental process, $\Delta\varepsilon$, expresses the orientational contribution to the dielectric permittivity through the Debye/Onsager model[21,22]

$$\epsilon_s - \epsilon_\infty = \frac{1}{3\epsilon_o} F \cdot g_K \cdot \frac{\mu_o^2}{k_B T} \cdot \frac{\rho}{M_{r.u.}} N_A \quad (6)$$

Here, μ_o is the dipole moment of the repeat unit in the gas phase, ρ is the mass density, $M_{r.u.}$ is the molar mass of the repeat unit (=0.142 kg mol^{-1}), N_A is the Avogadro number, and $F = (\varepsilon_s(\varepsilon_\infty + 2)^2)/(3(2\varepsilon_s + \varepsilon_\infty))$ is the Onsager factor (ε_s and ε_∞ are the low- and high-frequency values of dielectric permittivity, respectively) for polar but nonassociating molecules. Equation 6 contains a factor, g_K, not considered in the original Debye/Onsager theory. It was introduced later by Kirkwood and Fröhlich (known as the Kirkwood factor) to account for dipolar orientation correlations of interacting dipoles. Neighboring molecules that orient parallel or antiparallel have values $g_K > 1$ and $g_K < 1$, respectively. Employing $\mu_o = 0.7$ D for the dipole moment of syndiotactic units and $T\Delta\varepsilon_{\alpha1} \sim 525$ K results in $g_K \sim 2.7$, revealing strongly interacting segments with a parallel orientation.

Pressure-dependent DS studies were made based on the different pressure sensitivity of the segmental processes.[40−42] The results are summarized in Figure 7a,b, where the pressure and temperature dependence of the segmental dynamics is depicted. The P dependence of the relaxation times can be described by the pressure equivalent to the VFT equation[43]

$$\tau = \tau_o \exp\left[\frac{D_P P_o}{P_o - P}\right] \quad (7)$$

where τ_o is the segmental relaxation time at atmospheric pressure at a given temperature, D_P is a dimensionless parameter, and P_o is the pressure corresponding to the "ideal" glass. Interestingly, both processes (α_1 and α_2) exhibit a similar pressure dependence suggesting their strong coupling.

Informative is the pressure sensitivity of the segmental relaxations encoded in the apparent activation volume. The latter quantity can be obtained by the slope at each pressure as[40−42]

https://doi.org/10.1021/acsapm.2c00299
ACS Appl. Polym. Mater. 2022, 4, 3833−3843

$$\Delta V^{\#} = 2.303RT\left[\frac{\partial \log \tau}{\partial P}\right]_T \quad (8)$$

which relates to the volume of the underlying dynamic processes. As the apparent activation volume depends also on pressure ($\Delta V^{\#} = RTD_P P_o/(P_o - P)^2$), it can be obtained for both processes in the limit of $P \rightarrow 0.1$ MPa. The result is plotted in Figure 7c as a function of temperature. The corresponding quantity for the single segmental process of PCHMA is also included for comparison in a T_g-scaled plot.[39] At temperatures slightly above T_g, the activation volumes of the two processes are very high. By increasing the temperature, they fall rapidly and approach the repeat unit volume (129 cm^3 mol^{-1}) of PCHC at $T \sim T_g + 80$ K. Notice that the two processes (α_1 and α_2 in PCHC) have undistinguishable $\Delta V^{\#}$ values and similar temperature dependencies, confirming that they both reflect segmental relaxation of different stereoregular repeat units.

As a next step, we examine the pressure sensitivity of the glass temperature of the two segmental relaxations obtained through the isobaric and isothermal measurements and is presented in Figure 7d. It is well known that the glass temperature in glass-forming systems is an increasing function of pressure. The P and T dependences of T_g and P_g, respectively, can be described by the empirical equation as[44,45]

$$T_g(P) = T_g(0)\left(1 + \frac{\nu}{\mu}P\right)^{1/\nu} \quad (9)$$

with $T_g(0)$ being the glass temperature at atmospheric pressure and μ and ν being the fitting parameters. This equation was first proposed by Simon and Glatzel[44] to describe the melting of solid gases under pressure and subsequently employed by Andersson and Andersson to describe the $T_g(P)$ of glass-forming systems.[45] The two segmental modes experience similar $T_g(P)$ dependencies. The pressure sensitivity values of T_g in the limit of ambient pressure, that is, $dT_g/dP|_{P\rightarrow 0}$, are 418 and 389 K GPa^{-1} for α_1 and α_2 processes, respectively. These values are characteristic of polymers having a rigid backbone. Indeed, the pressure coefficients are intermediate to the ones found in PS (360 K GPa^{-1}) and bisphenol-A–polycarbonate (BPA–PC) (520 K GPa^{-1}).[40]

The temperature dependence of the relaxation times of the two segmental processes corresponding to different PCHC homopolymers is compared in Figure 8 at ambient pressure (0.1 MPa). As expected, the application of pressure restricts molecular motions and slows down the respective dynamic processes.

The molar mass dependence of the extracted glass temperature(s) (both defined at $t \sim 100$ s) from Figure 8 is shown in Figure 9. Both segmental processes are plotted in the figure. However, the process that couples to the specific heat and freezes at T_g is α_1. Hence, the data from the α_1 process were fitted with the Fox–Flory equation: $T_g(\mathrm{K}) = T_g^{\infty} - K/M_n$, resulting in $T_g^{\infty} = (398 \pm 5)$ K and $K = 156{,}500$ g mol^{-1}. As expected, the limiting value of T_g is higher than in earlier reports based on a single homopolymer. The glass temperature of the homopolymers is intermediate to PS and BPA–PC.[18]

A property of the segmental dynamics closely related to the liquid-to-glass formation is the fragility parameter or the steepness index, m. It is used to quantify the steepness in the temperature dependence of the segmental relaxation times as T_g is approached from higher temperatures. It is defined as $\vartheta \log \tau/\vartheta(T_g/T)|_{T=T_g}$, which is equivalent to the slope in the "fragility" plot of log τ versus T_g/T. The steepness index can also be calculated as

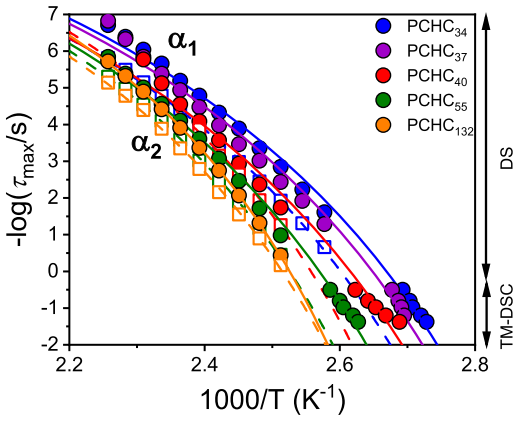

Figure 8. Arrhenius relaxation map for the segmental α_1 (filled symbols) and α_2 (open symbols) processes of PCHC homopolymers with different molar masses. Solid and dashed lines represent VFT fits to the faster and slower processes, respectively. Data points from DS and TM-DSC are indicated.

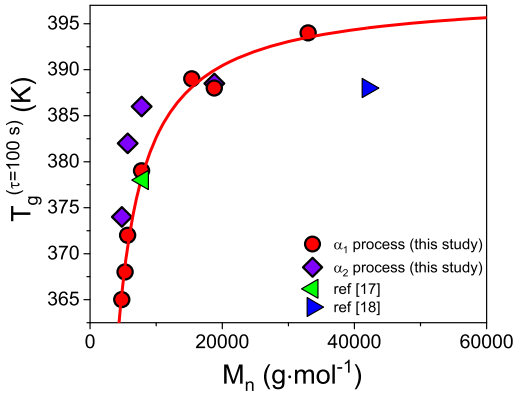

Figure 9. Molar mass dependence of the glass temperature of PCHC homopolymers. Data are obtained from DS (the glass temperature is operationally defined as the temperature where the dielectric loss maximum of the segmental processes is at 100 s). Additional literature data are included for comparison.[17,18]

$$m^* = \frac{BT_g}{2.303(T_g - T_o)^2} \quad (10)$$

The dependence of the relaxation times of the α_1 segmental process is shown in Figure 10a in a T_g-scaled plot as a function of T_g/T. The molar mass dependence of the steepness index is depicted in Figure 10b, as calculated from eq 10. PCHC exhibits an increasing fragility with increasing molar mass, as observed in a number of polymers. In the same figure (Figure 10b), we include fragility data for three related polymers: PS, poly(cyclohexyl ethylene) (PCHE), and PCHMA. They all display a similar molar mass dependence but with very different final values. Fragility values for PCHMA are the lowest, with those of PCHC being intermediate to PS and PCHMA. Experimental efforts first by Roland and co-workers[46,47] and Colucci et al.[48] and later by Kunal et al.[49] identified a relation of polymer fragility (low, intermediate, high) to molecular structure. They have shown that the relative rigidity of the side group and the backbone is an essential

https://doi.org/10.1021/acsapm.2c00299
ACS Appl. Polym. Mater. 2022, 4, 3833–3843

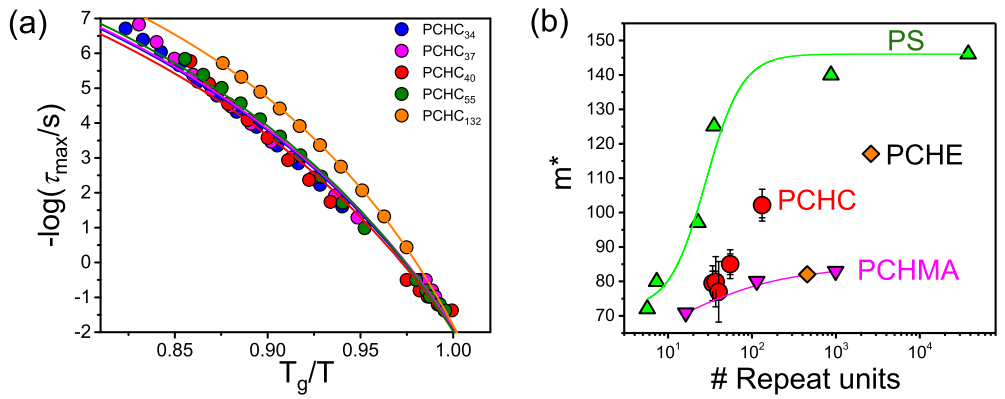

Figure 10. (a) Segmental relaxation times as a function of T_g/T for different molar masses of PCHC as indicated. (b) Fragility or steepness index as a function of the number of repeat units. The data refer to some structurally similar polymers: (spheres): PCHC, (up triangles): PS, (down triangles): PCHMA, and (rhombi): PCHE.

Table 3. Parameters of the Arrhenius Equation for the Glassy Processes in PCHC Homopolymers for the Different Molar Masses

	β-process		γ-process		δ-process	
sample	$-\log(\tau_o/s)^a$	E (kJ/mol)	$-\log(\tau_o/s)^a$	E (kJ/mol)	$-\log(\tau_o/s)^a$	E (kJ/mol)
$PCHC_{34}$	14	84.6 ± 0.4	14	60.0 ± 0.1	14	46.3 ± 0.4
$PCHC_{37}$	14	87.6 ± 0.4	14	58.5 ± 0.2	14	45.8 ± 0.3
$PCHC_{40}$	14	88.6 ± 0.5	14	59.2 ± 0.1	14	48.5 ± 0.1
$PCHC_{55}$	14	86.6 ± 0.4	14	58.8 ± 0.1	14	50.2 ± 0.1
$PCHC_{132}$	14	91 ± 2	14	72.2 ± 0.1	14	51.8 ± 0.1

[a]Value held fixed.

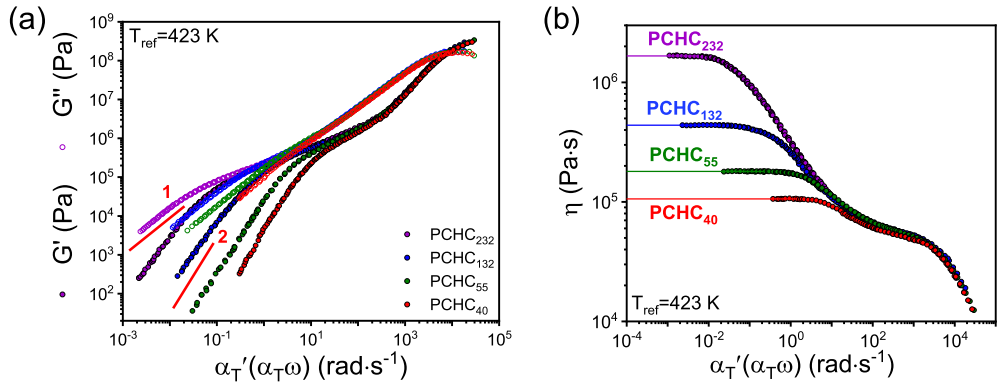

Figure 11. (a) Master curves of the storage (filled symbols) and loss (open symbols) shear moduli for $PCHC_{40}$ (red), $PCHC_{55}$ (green), $PCHC_{132}$ (blue), and $PCHC_{232}$ (purple) all at the same reference temperature of 423 K. The data are shifted horizontally with respect to the $PCHC_{132}$ data so as to coincide at the glass temperature. Lines with slopes of 1 and 2 are shown. (b) Complex viscosity as a function of angular frequency for the same PCHC homopolymers at the same reference temperature (423 K).

parameter governing the segmental dynamics of polymers. Subsequently, a generalized entropy theory by Dudowicz et al.[50] suggested a relation of fragility to the packing ability of chains. Chains with rigid backbones and bulky side groups have poorly packed chains that hence show higher fragilities. On the other hand, polymers with flexible chains pack better and exhibit lower fragilities. The polymers PS, PCHMA, and PCHC nicely show this behavior. Replacing the bulky side group in PS by the more flexible cyclohexyl group (in PCHC, PCHMA, and PCHE) undergoing intramolecular chair-to-chair conversion decreases the fragility.

Apart from the dual segmental process at temperatures in the vicinity of the respective T_g, additional processes are evident at lower temperatures, near ambient temperatures. Within the glassy state, the activation plot (Figure 6) exhibits three additional processes. The temperature dependence of the characteristic times for the β-, γ-, and δ-processes conform to an Arrhenius dependence

$$\tau = \tau_o \exp\left[\frac{E}{RT}\right] \tag{11}$$

where τ_o is the relaxation time in the limit of very high temperatures and E is the activation energy with parameters that are summarized in Table 3.

All three are of low dielectric strength (β process: $T\Delta\varepsilon = (9 \pm 1)$ K, $m \sim 0.5$, $mn \sim 0.4$; γ process: $T\Delta\varepsilon = (1.5 \pm 0.5)$ K, $m \sim 0.6$, $mn \sim 1$; δ process: $T\Delta\varepsilon = (55 \pm 3)$ K, $m \sim 0.4$, $mn \sim 0.2$). The δ-process is the most intense process in the glassy

https://doi.org/10.1021/acsapm.2c00299
ACS Appl. Polym. Mater. 2022, 4, 3833−3843

state. Its actual relaxation times and temperature dependence are in proximity to the relaxation of the cyclohexyl ring found in PCHMA. The latter is associated with the chair-to-chair conformational motion of the cyclohexyl ring (E = 47.5 kJ mol^{-1}).[31,36] The very weak γ-process with similar activation energy could reflect a more local motion of the cyclohexyl group. The presence of relaxation processes (that operate at ambient temperature) is normally associated with the mechanical properties (toughness). The weak β-process being in proximity to the main α_1 process is associated with the partial rotation (localized movement) of the carboxyl group. A similar relaxation process was observed in PCHMA.[38] Such sub-T_g processes are common among glass-forming polymers.[51,52]

Viscoelastic Properties. High T_g and tough materials require entangled chains. To test this, we employed rheology for the PCHC homopolymers with an emphasis on the viscoelastic response of the $PCHC_{232}$ homopolymer (M_n = 33,000 g mol^{-1}; $Đ$ = 1.56) with a much narrower distribution than in earlier studies.[18] The master curves of the storage and loss moduli of $PCHC_{40}$, $PCHC_{55}$, $PCHC_{132}$, and $PCHC_{232}$ are shown in Figure 11 at a reference of 423 K. The shift factors, a_T, are provided that are fitted to the WLF equation (the extracted parameters are discussed with respect to Figure S5, Supporting Information and in comparison to the VFT equation with respect to Figure S6). There is a small but systematic dependence of the WLF parameters on molar mass. The frequency dependence of the storage and loss moduli for the highest molar mass sample ($PCHC_{232}$) exhibits the segmental processes at higher frequencies, followed by a continuous decrease at intermediate frequencies, to the terminal process at lower frequencies. At the lower frequencies, the storage and loss moduli exhibit the typical Newtonian behavior ($G' \sim \omega^2$ and $G'' \sim \omega$). At intermediate frequencies, the storage and loss moduli approach each other without showing a plateau. It is known that the value of the plateau modulus, G_N°, provides the molar mass between entanglements, M_e, through $G_N^\circ = \rho RT/M_e$, where ρ is the density and R is the gas constant. Evidently, M_e cannot be extracted from the studied molar masses.

More informative is the molar mass dependence of the terminal times and of the zero shear viscosity, both depicted in Figure S7, Supporting Information. The molar mass dependence of the terminal relaxation times follows the scaling ($\tau_{NM}/\tau_{SM} \sim M^{3.2}$).[53,54] At the same time, the zero-shear viscosity scales as $\eta_o \sim M^{1.4}$ revealing an intermediate behavior between Rouse and entangled chains. The exponents, however, should be taken with caution because of the narrow range of molar masses. It is only for the PCHC homopolymer with the higher molar mass that a clear deviation occurs from the Rouse behavior suggesting the proximity to M_c. If M_c is taken at the point of deviation from the Rouse regime (i.e., around 33,000 g mol^{-1}), then a lower estimate of M_e would be at ∼16,000 g mol^{-1} in line with an earlier estimate from a more polydisperse sample.[18] However, given the lack of a plateau in the master curve for this sample, it is certain that M_e is higher than 16,000 g mol^{-1}. This situation can be contrasted with two high T_g polymers, PS and BPA−PC, with respective M_es of 16,600 and 1600 g mol^{-1}.[54] Hence, although PCHC is a high T_g material, the lack of entanglements makes it brittle at least for molar masses in the range of the present investigation.

CONCLUSIONS

A series of stereoregular PCHC homopolymers with molar masses in the range from 4800 to 33,000 g mol^{-1} and with relatively narrow dispersities were synthesized via copolymerization of CHO and carbon dioxide using CoSalen and [PPN]Cl as the catalyst. The molecular dynamics of the homopolymers was investigated for the first time with DS as a function of temperature and pressure. Well into the glassy state, the dynamics reflects the cyclohexyl group motion with an activation energy of ∼50 kJ mol^{-1}, also found in PCHMA. This motion, acting also at ambient temperature, is facilitated by the main chain ester group, as shown by its high dielectric strength.

The molecular dynamics in the vicinity of the liquid-to-glass temperature was very complex. The dual segmental processes were inseparable by decreasing temperature or by increasing pressure. Based on DFT calculations of the dipole moments, they were ascribed to different stereo sequences of the PCHC backbone. From the two processes, it is only the faster one (α_1 process) that couples to the heat capacity. This process has a molar mass dependence that can be described by the Fox−Flory equation. The predicted glass temperature in the limit of very high molar masses is ∼398 K. This limiting value is intermediate to PS and BPA−PC homopolymers. The high T_g value obtained herein justifies its application as a CO_2-based alternative for PS in block copolymers. Moreover, fragility increased with increasing molar mass, an expectation born from rigid and bulky polymers. The limiting fragility values were intermediate to PS and PCHMA. The flexible cyclohexyl group in PCHC (and PCHMA) undergoing intramolecular chair-to-chair conversion increases the packing ability and consequently decreases the fragility.

The molar mass dependence of the terminal relaxation times and the zero-shear viscosity with respective dependencies as $\tau_{NM}/\tau_{SM} \sim M^{3.2}$ and $\eta_o \sim M^{1.4}$ reveal an intermediate behavior between Rouse and entangled chains. Overall, the data are suggesting that M_e is well-above 16,000 g mol^{-1}, which plays a key role when aiming at the application of PCHC as a more sustainable replacement for PS. Although PCHC is a high T_g material, the lack of entanglements makes it brittle, at least for molar masses in the range of the present investigation. Efforts in the CO_2 synthesis of PCHC should be directed at even higher molar masses in excess of 50,000 g mol^{-1}.

ASSOCIATED CONTENT

Supporting Information

The Supporting Information is available free of charge at https://pubs.acs.org/doi/10.1021/acsapm.2c00299.

Details on the synthesis (^{1}H and ^{13}C inverse-gated NMR spectra of $PCHC_{108}$); additional DS data (including fitting procedure of DS data); rheology shift factors and WLF coefficients as a function of molar mass; molar mass dependence of terminal relaxation times; and cartesian coordinates of minimized structures (PDF)

AUTHOR INFORMATION

Corresponding Authors

Holger Frey − *Department of Chemistry, Johannes Gutenberg Universität Mainz, 55099 Mainz, Germany;* orcid.org/0000-0002-9916-3103; Email: hfrey@uni-mainz.de

George Floudas − *Department of Physics, University of Ioannina, 45110 Ioannina, Greece; Max Planck Institute for*

https://doi.org/10.1021/acsapm.2c00299
ACS Appl. Polym. Mater. 2022, 4, 3833−3843

Polymer Research, 55128 Mainz, Germany; University Research Center of Ioannina (URCI)—Institute of Materials Science and Computing, 45110 Ioannina, Greece; orcid.org/0000-0003-4629-3817; Email: gfloudas@uoi.gr

Authors

Marianna Spyridakou − *Department of Physics, University of Ioannina, 45110 Ioannina, Greece*

Christina Gardiner − *Department of Chemistry, Johannes Gutenberg Universität Mainz, 55099 Mainz, Germany*

George Papamokos − *Department of Physics, University of Ioannina, 45110 Ioannina, Greece;* orcid.org/0000-0002-7671-2798

Complete contact information is available at: https://pubs.acs.org/10.1021/acsapm.2c00299

Notes

The authors declare no competing financial interest.

■ ACKNOWLEDGMENTS

This research was supported by the Hellenic Foundation for Research and Innovation (H.F.R.I.) under the "First Call for H.F.R.I. Research Projects to support Faculty members and Researchers and the procurement of high-cost research equipment grant" (Project Number: 183). M.S. was financially supported by the program "PERIFEREIAKI ARISTEIA" (Regional Excellence) cofinanced by the European Union and the Hellenic Republic Ministry of development and investments under NSRF 2014−2020 (Region of Epirus, call 111).

■ REFERENCES

(1) Inoue, S.; Koinuma, H.; Tsuruta, T. Copolymerization of Carbon Dioxide and Epoxide with Organometallic Compounds. *Makromol. Chem.* **1969**, *130*, 210−220.

(2) Cohen, C. T.; Thomas, C. M.; Peretti, K. L.; Lobkovsky, E. B.; Coates, G. W. Copolymerization of Cyclohexene Oxide and Carbon Dioxide Using (salen) Co (III) Complexes: Synthesis and Characterization of Syndiotactic Poly(cyclohexene carbonate). *Dalton Trans.* **2006**, 237−249.

(3) Hsu, T.-J.; Tan, C.-S. Synthesis of Polyethercarbonate from Carbon Dioxide and Cyclohexene Oxide by Yttrium−metal Coordination Catalyst. *Polymer* **2001**, *42*, 5143−5150.

(4) Kember, M. R.; Williams, C. K. Efficient Magnesium Catalysts for the Copolymerization of Epoxides and CO_2; Using Water to Synthesize Polycarbonate Polyols. *J. Am. Chem. Soc.* **2012**, *134*, 15676−15679.

(5) Wu, G.-p.; Jiang, S.-d.; Lu, X.-b.; Ren, W.-m.; Yan, S.-k. Stereoregular Poly(cyclohexene carbonate)s: Unique Crystallization Behavior. *Chin. J. Polym. Sci.* **2012**, *30*, 487−492.

(6) Sulley, G. S.; Gregory, G. L.; Chen, T. T. D.; Peña Carrodeguas, L.; Trott, G.; Santmarti, A.; Lee, K.-Y.; Terrill, N. J.; Williams, C. K. Switchable Catalysis Improves the Properties of CO_2-Derived Polymers: Poly(cyclohexene carbonate-b-ε-decalactone-b-cyclohexene carbonate) Adhesives, Elastomers, and Toughened Plastics. *J. Am. Chem. Soc.* **2020**, *142*, 4367−4378.

(7) Darensbourg, D. J.; Mackiewicz, R. M.; Phelps, A. L.; Billodeaux, D. R. Copolymerization of CO_2 and Epoxides Catalyzed by Metal Salen Complexes. *Acc. Chem. Res.* **2004**, *37*, 836−844.

(8) Zhang, D.; Zhang, H.; Hadjichristidis, N.; Gnanou, Y.; Feng, X. Lithium-Assisted Copolymerization of CO_2 /Cyclohexene Oxide: A Novel and Straightforward Route to Polycarbonates and Related Block Copolymers. *Macromolecules* **2016**, *49*, 2484−2492.

(9) Jia, M.; Hadjichristidis, N.; Gnanou, Y.; Feng, X. Monomodal Ultrahigh-Molar-Mass Polycarbonate Homopolymers and Diblock Copolymers by Anionic Copolymerization of Epoxides with CO_2. ACS Macro Letters, 8(12. *ACS Macro Lett.* **2019**, *8*, 1594−15981.

(10) Yang, G.-W.; Wu, G.-P. High-Efficiency Construction of CO_2-Based Healable Thermoplastic Elastomers via a Tandem Synthetic Strategy. *ACS Sustainable Chem. Eng.* **2019**, *7*, 1372−1380.

(11) Reiter, M.; Kronast, A.; Kissling, S.; Rieger, B. In Situ Generated ABA Block Copolymers from CO_2 , Cyclohexene Oxide, and Poly(dimethylsiloxane)s. *ACS Macro Lett.* **2016**, *5*, 419−423.

(12) Kember, M. R.; Copley, J.; Buchard, A.; Williams, C. K. Triblock Copolymers from Lactide and Telechelic Poly(cyclohexene carbonate). *Polym. Chem.* **2012**, *3*, 1196−1201.

(13) Bailer, J.; Feth, S.; Bretschneider, F.; Rosenfeldt, S.; Drechsler, M.; Abetz, V.; Schmalz, H.; Greiner, A. Synthesis and Self-assembly of Biobased Poly(limonene carbonate)-block-poly(cyclohexene carbonate) Diblock Copolymers Prepared by Sequential Ring-Opening Copolymerization. *Green Chem.* **2019**, *21*, 2266−2272.

(14) Zhang, Y.-Y.; Wu, G.-P.; Darensbourg, D. J. CO_2-Based Block Copolymers: Present and Future Designs. *Trends Chem.* **2020**, *2*, 750−763.

(15) Scharfenberg, M.; Hilf, J.; Frey, H. Functional Polycarbonates from Carbon Dioxide and Tailored Epoxide Monomers: Degradable Materials and their Application Potential. *Adv. Funct. Mater.* **2018**, *28*, 1704302.

(16) Scharfenberg, M.; Hofmann, S.; Preis, J.; Hilf, J.; Frey, H. Rigid Hyperbranched Polycarbonate Polyols from CO2 and Cyclohexene-Based Epoxides. *Macromolecules* **2017**, *50*, 6088−6097.

(17) Thorat, S. D.; Phillips, P. J.; Semenov, V.; Gakh, A. Physical Properties of Aliphatic Polycarbonates Made from CO_2 and Epoxides. *J. Appl. Polym. Sci.* **2003**, *89*, 1163−1176.

(18) Koning, C.; Wildeson, J.; Parton, R.; Plum, B.; Steeman, P.; Darensbourg, D. J. Synthesis and Physical Characterization of Poly(cyclohexane carbonate), Synthesized from CO_2 and Cyclohexene Oxide. *Polymer* **2001**, *42*, 3995−4004.

(19) Ford, D. D.; Nielsen, L. P. C.; Zuend, S. J.; Musgrave, C. B.; Jacobsen, E. N. Mechanistic Basis for High Stereoselectivity and Broad Substrate Scope in the (salen) Co (III)-catalyzed Hydrolytic Kinetic Resolution. *J. Am. Chem. Soc.* **2013**, *135*, 15595−15608.

(20) Hensel, A.; Dobbertin, J.; Schawe, J. E. K.; Boller, A.; Schick, C. Temperature-Modulated Calorimetry and Dielectric Spectroscopy in the Glass Transition Region of Polymers. *J. Therm. Anal.* **1996**, *46*, 935−954.

(21) Kremer, F.; Schoenhals, A. *Broadband Dielectric Spectroscopy*; Springer: Berlin, 2002.

(22) Floudas, G. *Dielectric Spectroscopy*; Matyjaszewski, K., Möller, M., Eds.; Elsevier BV: Amsterdam, 2012; Vol. *232*, pp 825−845.

(23) Havriliak, S.; Negami, S. A Complex Plane Representation of Dielectric and Mechanical Relaxation Processes in Some Polymers. *Polymer* **1967**, *8*, 161−210.

(24) Chai, J.-D.; Head-Gordon, M. Long-range Corrected Hybrid Density Functionals with Damped Atom-atom Dispersion Corrections. *Phys. Chem. Chem. Phys.* **2008**, *10*, 6615−6620.

(25) Yoshida, N.; Aoki, D.; Sasanuma, Y. Configurational Statistics of Poly(cyclohexene carbonate). *Macromolecules* **2020**, *53*, 9362−9374.

(26) Frisch, M. J.; Trucks, G. W.; Schlegel, H. B.; Scuseria, G. E.; Robb, M. A.; Cheeseman, J. R.; Scalmani, G.; Barone, V.; Petersson, G. A.; Nakatsuji, H.; Li, X.; Caricato, M.; Marenich, A. V.; Bloino, J.; Janesko, B. G.; Gomperts, R.; Mennucci, B.; Hratchian, H. P.; Ortiz, J. V.; Izmaylov, A. F.; Sonnenberg, J. L.; Williams-Young, D.; Ding, F.; Lipparini, F.; Egidi, F.; Goings, J.; Peng, B.; Petrone, A.; Henderson, T.; Ranasinghe, D.; Zakrzewski, V. G.; Gao, J.; Rega, N.; Zheng, G.; Liang, W.; Hada, M.; Ehara, M.; Toyota, K.; Fukuda, R.; Hasegawa, J.; Ishida, M.; Nakajima, T.; Honda, Y.; Kitao, O.; Nakai, H.; Vreven, T.; Throssell, K.; Montgomery, J. A., Jr.; Peralta, J. E.; Ogliaro, F.; Bearpark, M. J.; Heyd, J. J.; Brothers, E. N.; Kudin, K. N.; Staroverov, V. N.; Keith, T. A.; Kobayashi, R.; Normand, J.; Raghavachari, K.; Rendell, A. P.; Burant, J. C.; Iyengar, S. S.; Tomasi, J.; Cossi, M.; Millam, J. M.; Klene, M.; Adamo, C.; Cammi, R.; Ochterski, J. W.;

Martin, R. L.; Morokuma, K.; Farkas, O.; Foresman, J. B.; Fox, D. J. *Gaussian 16, R.A.03*; Gaussian, Inc.: Wallingford CT, 2016.
(27) Lu, X.-B.; Darensbourg, D. J. Cobalt Catalysts for the Coupling of CO_2 and Epoxides to Provide Polycarbonates and Cyclic Carbonates. *Chem. Soc. Rev.* **2012**, *41*, 1462−1484.
(28) Theodoridis, A.; Papamokos, G.; Wiesenfeldt, M. P.; Wollenburg, M.; Müllen, K.; Glorius, F.; Floudas, G. Polarity Matters: Dielectric Relaxation in All-cis-Multifluorinated Cycloalkanes. *J. Phys. Chem. B* **2021**, *125*, 3700−3709.
(29) Donth, E. *The Glass Transition*; Springer-Verlag: Berlin, Heidelberg, 2001.
(30) Ishida, Y.; Yamafuji, K. Studies on Dielectric Behaviors in a Series of Polyalkyl-Methacrylates. *Kolloid J* **1961**, *177*, 97.
(31) Heijboer, J. Mechanical Properties of Glassy Polymers Containing Saturated Rings, Ph.D. Thesis, University of Leiden, 1972.
(32) Frosini, V.; Magagnini, P.; Butta, E.; Baccaredda, M. Secondary Mechanical Relaxation Effects in Some Cycloalkyl Side Groups Containing Polymers. *Kolloid-Z.* **1966**, *213*, 115.
(33) Ribes-Greus, A.; Gomez-Ribelles, J. L.; Diaz-Calleja, R. Dielectric and Mechanical-Dynamical Studies on Poly(cyclohexyl methacrylate). *Polymer* **1985**, *26*, 1849.
(34) Laupretre, F.; Virlet, J.; Bayle, J. P. Local Motions between Unequivalent Conformations in Solid Poly(cyclohexyl methacrylate): A Variable-Temperature Magic-Angle Carbon-13 Nuclear Magnetic Resonance Study. *Macromolecules* **1985**, *18*, 1846.
(35) Fytas, G. Relaxation Processes in Amorphous Poly(cyclohexyl methacrylate) in the Rubbery and Glassy State Studied by Photon Correlation Spectroscopy. *Macromolecules* **1989**, *22*, 211.
(36) Floudas, G.; Fytas, G.; Fischer, E. W. Relaxation Processes in a Poly(cyclohexy1 methacrylate) /Additive System As Studied by Photon Correlation, Dielectric Relaxation, and Mechanical Relaxation Spectroscopy. *Macromolecules* **1991**, *24*, 1955−1961.
(37) Fytas, G.; Floudas, G.; Ngai, K. L. Density and Concentration Fluctuations in Plasticized Poly(cyclohexyl methacrylate). *Macromolecules* **1990**, *23*, 1104.
(38) Murthy, S. S. N.; Shahin, M. A Note on 'Sub-T_g Relaxation Processes in Poly(cyclohexylmethacrylate). *Eur. Polym. J.* **2006**, *42*, 715−720.
(39) Roland, C. M.; Casalini, R. Dynamics of Poly(cyclohexyl methacrylate): Neat and in Blends with Poly(α-methylstyrene). *Macromolecules* **2007**, *40*, 3631−3639.
(40) Floudas, G.; Paluch, M.; Grzybowski, A.; Ngai, K. *Molecular Dynamics of Glass-Forming Systems—Effects of Pressure*; Springer Verlag: Berlin, 2010.
(41) Floudas, G.; Reisinger, T. Pressure Dependence of the Local and Global Dynamics of Polyisoprene. *J. Chem. Phys.* **1999**, *111*, 5201−5204.
(42) Floudas, G.; Fytas, G.; Reisinger, T.; Wegner, G. Pressure-Induced Dynamic Homogeneity in an Athermal Diblock Copolymer Melt. *J. Chem. Phys.* **1999**, *111*, 9129−9132.
(43) Paluch, M.; Patkowski, A.; Fischer, E. W. Temperature and Pressure Scaling of the α Relaxation Process in Fragile Glass Formers: A Dynamic Light Scattering Study. *Phys. Rev. Lett.* **2000**, *85*, 2140.
(44) Simon, F.; Glatzel, G. Bemerkungen zur Schmelzdruckkurve. *Anorg. Allg. Chem.* **1929**, *178*, 309.
(45) Andersson, S. P.; Andersson, O. Relaxation Studies of Poly(propylene glycol) under High Pressure. *Macromolecules* **1998**, *31*, 2999.
(46) Ngai, K. L.; Roland, C. M. Chemical Structure and Intermolecular Cooperativity: Dielectric Relaxation Results. *Macromolecules* **1993**, *26*, 6824−6830.
(47) Santangelo, P. G.; Roland, C. M. Molecular Weight Dependence of Fragility in Polystyrene. *Macromolecules* **1998**, *31*, 4581−4585.
(48) Colucci, D. M.; McKenna, G. B. Fragility of Polymeric Liquids: Correlations Between Thermodynamic and Dynamic Properties. *MRS Online Proc. Libr.* **1997**, *455*, 171.
(49) Kunal, K.; Robertson, C. G.; Pawlus, S.; Hahn, S. F.; Sokolov, A. P. Role of Chemical Structure in Fragility of Polymers: A Qualitative Picture. *Macromolecules* **2008**, *41*, 7232−7238.
(50) Dudowicz, J.; Freed, K. F.; Douglas, J. F. Fragility of Glass-Forming Polymer Liquids. *J. Phys. Chem. B* **2005**, *109*, 21350−21356.
(51) Mpoukouvalas, K.; Floudas, G.; Williams, G. Origin of the α, β, ($\beta\alpha$), and "Slow" Dielectric Processes in Poly(ethyl methacrylate). *Macromolecules* **2009**, *42*, 4690−4700.
(52) Spyridakou, M.; Maji, T.; Gkikas, M.; Ngai, K. L.; Floudas, G. Sub-Rouse Dynamics in Poly(isobutylene) as a Function of Molar Mass. *Macromolecules* **2021**, *54*, 9091−9099.
(53) Rouse, P. E. A Theory of Linear Viscoelastic Properties of Dilute Solutions of Coiling Polymers. *J. Chem. Phys.* **1953**, *21*, 1272.
(54) Fetters, L. J.; Lohse, D. J.; Colby, R. H. *Physical Properties of Polymers Handbook 2e*; Springer, 2006.

https://doi.org/10.1021/acsapm.2c00299
ACS Appl. Polym. Mater. 2022, 4, 3833−3843